MODELLING AIR-SOURCE HEAT PUMPS IN COLD CLIMATIC CONDITIONS CONSIDERING THE EFFECTS OF FROSTING

Siddhartha Gollamudi[1*], Easwaran Krishnana[1], Hadi Ramin[1], Gurubalan Annadurai[2], Carey Simonson[1]

[1]Department of Mechanical Engineering, University of Saskatchewann, Saskatoon, Canada

[2] Department of Energy Science and Engineering, IIT Bombay, Mumbai, India.

[*]Correponding author, E-mail address: bqm075@usask.ca

ABSTRACT

The world is fastly adopting building electrification to reduce buildings' greenhouse gas (GHG) emissions. Air Source Heat Pumps (ASHPs) are cleaner and more efficient than fossil fuel-based systems like furnaces and boilers for heating buildings. The performance of ASHP is highly dependent on climatic conditions(i.e. ambient temperature and humidity). When the ambient air temperature drops below the sub-zero region, ASHPs face the problems of frosting and high compression ratios. The present study investigates the effects of such issues on the performance of an ASHP in Saskatoon, Canada. The performance of the ASHP is presented in terms of the Coefficient of Performance (COP), and the effects of condensation temperature and frosting on COP are investigated. It is observed that the COP drops with the decrease in ambient air temperature. Furthermore, an increase in condensation temperature limits the operating range of an ASHP. The greenhouse gas (GHG) emissions from ASHP are compared with natural gas heating to determine the environmental impact.

INTRODUCTION

Buildings consume about 30% of the energy consumed around the globe (Abergel & Delmastro), (Krishnan et al., 2019) and about 40% in developed countries (Krishnan et al., 2021). Heating ventilation and air-conditioning (HVAC) systems essential for maintaining indoor thermal comfort consume about 55% of the building's energy consumption (Ramin et al., 2019), and heating systems specifically account for 12% of global CO_2 emissions (IEA, 2019). Therefore, transitioning from fossil-fuel-based heating systems like boilers and furnaces to cleaner solutions is an essential and practical approach to mitigate greenhouse gas (GHG) emissions from buildings. Air-source heat pumps (ASHPs) are heat (and cooling) systems that operate on electricity and are more efficient and eco-friendly than fossil-fuel-based systems, provided that electricity is generated from clean sources. The Coefficient of Performance of ASHP is greater than 1, meaning that ASHPs produce multiple units of heating/ cooling output for one unit of input. On the contrary, fossil-fuel systems have a COP in the range of 0.75-0.85 (Staffell et al., 2012).

ASHPs face performance deterioration in cold climates. The degradation is due to frosting and high compression ratios. The moisture in the air freezes on the evaporator when the evaporator temperature falls below 0℃ and the dew-point temperature of ambient air. Frosting decreases the evaporator heat transfer rate and deteriorates performance. Regular defrosting cycles are needed to maintain the operation of ASHP. Defrosting methods include reverse cycle defrosting (RCD) (Huang et al., 2009), electric defrost (Zhao et al., 2020), and hot-gas bypass (HGB) (Hu et al., 2015) methods. Extensive research has been carried out to improve the defrosting techniques and also develop no-frost strategies such as thermal energy storage (Dong et al., 2015), inlet air-dehumidification (Su et al., 2017), solar assistance[9], etc. During a frosting-defrosting cycle, the heat pump's performance decreases gradually during frost build-up. Furthermore, after considerable frost build-up defrosting cycle starts to consume energy to melt frost and is also associated with transient losses (Dongellini et al., 2017.), which needs to be accounted for in feasibility studies to determine the efficacy of ASHP accurately.

A typical air-source heat pump is shown in Fig.1. The evaporator (outdoor unit) is used to extract heat from the ambient and supply it indoors using a condenser (indoor unit). The evaporation temperature is always lower than ambient air to facilitate heat transfer from ambient air to the evaporator. As ambient air temperature drops, the evaporator temperature and pressure also drop, increasing the compression ratio (ratio of condenser pressure to evaporator pressure) (Cabrol & Rowley, 2012; Liu et al., 2017). High compression ratios decrease the efficiency of the compressor resulting in lower COP and high refrigerant discharge temperatures at the compressor. The refrigerant discharge temperature at the outlet of the compressor should be limited to 115℃ to ensure the safe operation of the compressor (Sun et al., 2021). Substantial research in fields of cascade cycles (Boahen & Choi, 2019), two-stage vapour injection heat pumps (Bertsch & Groll, 2008), thermal energy storage (Lin et al., 2022), solar assistance (Yang et al., 2021), exhaust air heat pumps (Li et al., 2022), and refrigerant mixtures (Rajapaksha, 2005) has been carried out to reduce compression ratio and aid cold climate operation of ASHPs

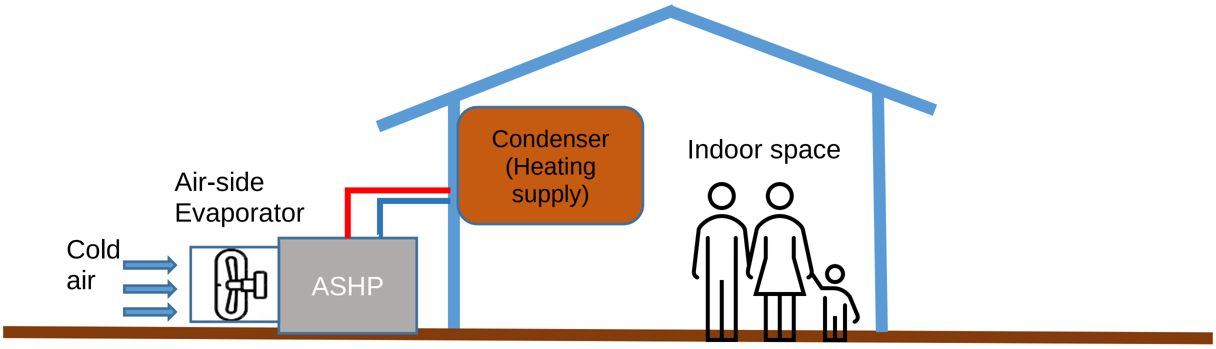

Figure 1: Air-source heat pump layout

Frosting and high compression ratios occur at different operating intervals. Frosting is primarily observed when the ambient temperature is between -15℃ to 6℃ and relative humidity is upwards of 50% [19], and high compression ratios are observed when the ambient air temperature drops below -15℃. Therefore, it becomes essential to study the combined influence of frosting and compression ratios on standard ASHP before making an informed choice on the type of modification to implement to aid cold climate operation.

The present study analyses the effect of ambient temperature and relative humidity on the performance of an ASHP operating in Saskatoon, Canada. The winters in Saskatoon are harsh, and the temperatures are below zero for 37% of the year. Furthermore, the emissions from the ASHP are evaluated against conventional natural gas boilers to determine if a large-scale retrofit is feasible to reduce GHG emissions from building heating systems in Saskatoon.

METHODOLOGY

To investigate the performance and GHG emissions of an ASHP in Saskatoon, the thermodynamic model of an ASHP is modelled to meet the building heating loads generated from TRNSYS for a small office building according to the following assumptions [20-22]:

- Heat losses and pressure drops in the refrigerant flow lines and heat pump components are neglected.
- Throttling is an isenthalpic process
- The refrigerant exits the evaporator in a gaseous form with a superheating degree of 5K
- The refrigerant leaves the condenser in a liquid form with a subcooling degree of 3K
- The effectiveness of the heat exchangers is 0.75

Energy balance equations form the basis of the thermodynamic model. Eq. 1-8 represent the energy balance equations for the evaporator, compressor, condenser, and expansion valve.

Evaporator

$$\dot{Q}_{ev} = \dot{m}_r\left(h_{ev_{out}} - h_{ev_{in}}\right) \tag{1}$$

$$\dot{Q}_{ev\_max} = \dot{m}_a c_a (T_a - T_{ev}) \tag{2}$$

$$\dot{Q}_{ev} = \varepsilon \dot{Q}_{max} \tag{3}$$

Condenser

$$\dot{Q}_{con} = \dot{m}_r (h_{con\_in} - h_{con\_out}) \tag{4}$$

Compressor

$$W_{comp} = \frac{\dot{m}_r (h_{con\_in} - h_{ev\_out})}{\eta_{isentopic} * \eta_{system}} \tag{5}$$

$$W_{comp} = \dot{m}_r(h_{con\_in} - h_{ev\_out}) \quad (6)$$

$$\eta_{isentopic} = f(P_{ev}, P_{con}) \quad (7)$$

The η_{system} is the combination of electrical and mechanical efficiency and is equal to 0.8.

Expansion valve

$$\text{h}_{exp\_in} = h_{exp\_out} \quad (8)$$

The COP of the ASHP is calculated using equations (9-10)

$$\text{COP}_{\text{no frost}} = \frac{\dot{Q}_{con}}{W_t} \quad (9)$$

$$W_t = W_{comp} + W_{fan} \quad (10)$$

Frost modelling

The frosting map of a typical ASHP is shown in Fig. 2 (Zhu et al., 2015). The frosting map is classified into five regions depending on the ambient temperature and relative humidity. The effects of frosting below -15℃ are neglected as the amount of moisture present in the air at such temperatures is very small and does not severely affect the performance of ASHP(Shao et al., 2021). To account for the performance loss during frosting and defrosting operations, the COP of the ASHP is modified using the corrections factors as shown in Table 1 and equation 11.

Table 1: Frosting correction factors (Cf) for different zones presented in Fig. 2 (Shao et al., 2021)

Frosting region	Cf value
E	0.9
D	0.86
C	0.8
B	0.74
A	0.68

$$\text{COP}_{\text{frosting}} = \text{COP}_{\text{no frost}} * \text{C}_{\text{f}} \quad (11)$$

Building heating loads

TRNSYS software is used to simulate the building heating loads, which the ASHP thermodynamic model uses to calculate the annual performance of the ASHP. The building considered in this study is a commercial building with a floor area of 510m^2 (Torcellini et al., 2008), and its thermal characteristics are as in Table. 2.

Table 2: Building envelope values used in TRNSYS simulation (Eldeeb, 2014)

Component	U-value (W/m^{2}K)
Wall	0.204
Roof	0.252
Floor	0.279

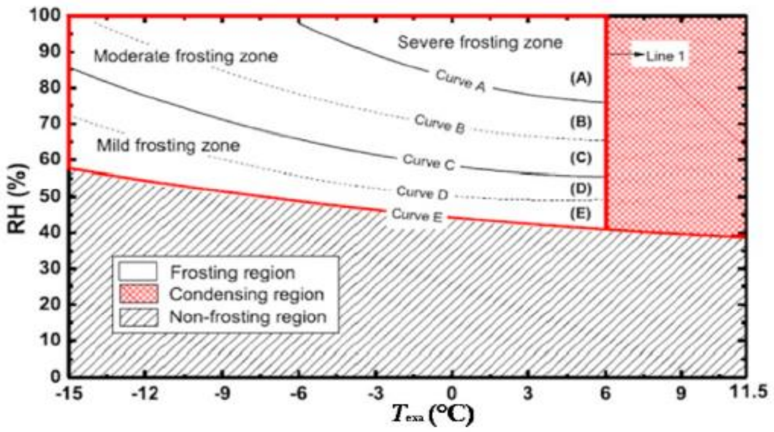

Figure 2: Frosting map under different operating conditions (Zhu et al., 2015)

GHG emissions

GHG gasses like CO2, SO2, NO2, and other organic chemicals are released when fossil fuels are burned. Equivalent CO2e is the emission measuring metric that collectively aggregates the emission from all the gases into a CO2 equivalent (Asaee et al., 2017). The electricity grid's GHG intensities are used to calculate the annual GHG emissions based on the electricity that ASHPs consume. The GHG intensity of the electric grid from SaskPower in 2020 was 0.53 kg CO2e/kWh and 0.24 kg CO2e/kWh for natural gas heating systems (City of Regina, 2020).

RESULTS AND DISCUSSION

The following section discusses the annual performance of ASHP and the effects of frosting on the performance of ASHP. Furthermore, the number of hours during which the ASHP cannot operate because of high discharge numbers is analyzed for different condensation temperatures. Auxiliary heating is used to cover the heating load during the non-operational hours of the ASHP. Finally, the GHG emissions from the ASHP operation are investigated and compared with that of natural gas heating.

Performance of ASHP in Saskatoon

An ASHP is simulated for one year (with a time-step of one hour) to meet the heating demand of the small office building, as described in the previous section. As depicted in Fig. 3, the COP of the ASHP system increases with the increase in ambient temperatures. The rise in COP is due to decreased compression ratios. An increase in COP directly results from higher isentropic efficiencies at low compression ratios.

Increasing condensation pressure leads to high compression ratios and discharge temperatures. Furthermore, the discharge temperature of the refrigerant in ASHP is limited to approximately 115℃. Therefore, an increase in condenser pressure decreases the ability of ASHP to operate at lower ambient temperature ranges, as seen in Fig. 3. As the condensation temperature increase from 30℃ to 50℃ the operational limit of ASHP diminishes from -36℃ to -20℃ ambient temperature. Fig. 4 illustrates the number of non-operational hours in each heating season where the discharge temperature exceeds 115℃ . The non-operative hours increase with the rise of condensation temperature.

There is a drop in COP as the ambient temperature approaches -15℃, as seen in Fig. 3 since the effects of frosting become significant from -15℃ to 6℃. Frosting-defrosting cycles increase the energy consumption by 11% when the heat is supplied at a 30℃ condensation temperature and about 20% when ASHP operates at a condensation temperature of 50℃. The difference in frosting energy consumption is as, at 30℃ condensation temperature, the operational envelope is relatively larger, extending to an ambient temperature of -36℃ compared to -20℃ ambient temperature at 50℃ condensation temperature. Since the effects of frosting are negligible above -15℃, the increase in energy consumption is more pronounced for 50℃ condensation temperature.

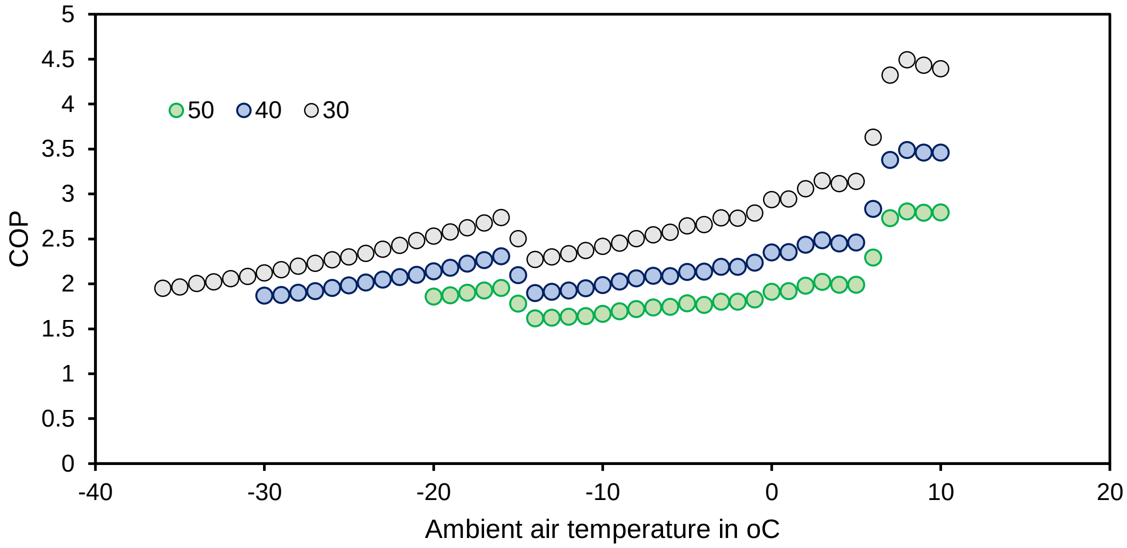

Figure 3: COP variation with ambient air temperature for condensation temperatures of 30℃, 40℃, and 50℃.

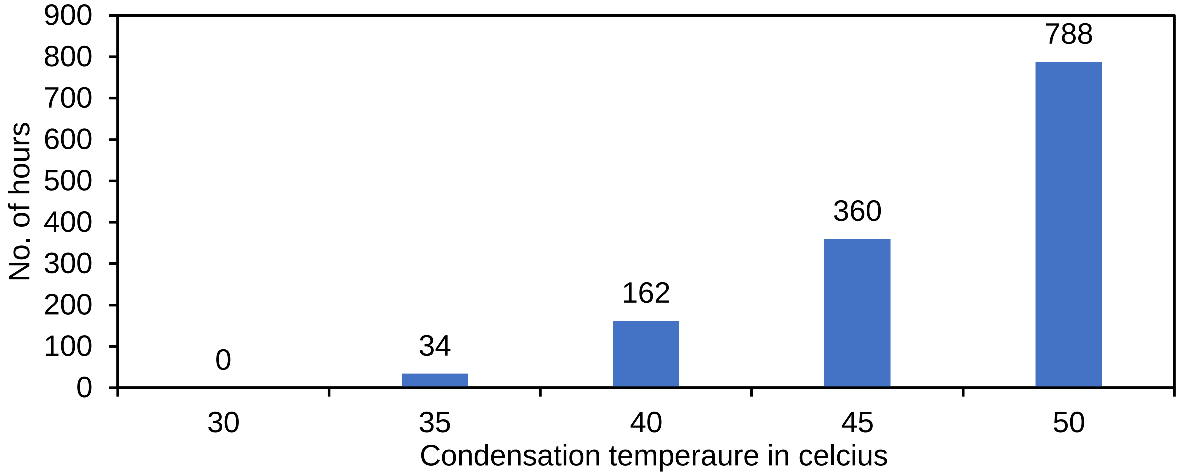

Figure 4: Number of hours where the discharge temperature exceeds 115℃ for condensation temperatures 30℃- 50℃

<u>GHG emissions</u>

High discharge temperatures limit the heat pump operation, as discussed in the section above. Therefore, auxiliary heating systems such as electric or natural gas are needed to cover the heating load during the non-operational hours of the ASHP. ASHP + electric auxiliary, ASHP + natural gas auxiliary, and the base case of natural gas heating are the three heating methods under investigation for GHG emissions; Fig. 5 demonstrates the control strategy of heating system operation. The condensation temperature of the ASHP is set to be 50℃ to perform the GHG emission comparison study

Table. 3 compares the GHG emissions for the three heating modes under consideration in the present study. The total heat demand of the building throughout the year is 70.15 MWh, 63%, i.e., the ASHP supplies 44.2 MWh while the remaining is provided by auxiliary heating. The average COP of the ASHP during its period of operation is 1.77. Therefore, the ASHP would consume about 24.9 MWh of energy. The COPs of natural gas and electric heating are 0.85 and 1, respectively and they supply remaining of the 25.9 MWh of heating demand.

It is evident from Table. 3 that a large-scale retrofit of ASHPs in the city of Saskatoon would increase the amount of GHG emissions. The unfavourability is mainly because of the low performance of ASHPs in cold climates and the GHG emission intensities of the electric grid. The all-electric system emits 39% more emissions than the conventional natural gas system, while ASHP + natural gas auxiliary increases emission by 5% from the base case. However, the GHG intensity of the electric grid is projected to reduce in the future as Saskatoon is trying to decarbonize the electricity grid by switching to wind and solar power (Saskatoon's Actions for Climate Change Mitigation, 2019). Reduction in GHG emissions will favour the ASHP retrofit.

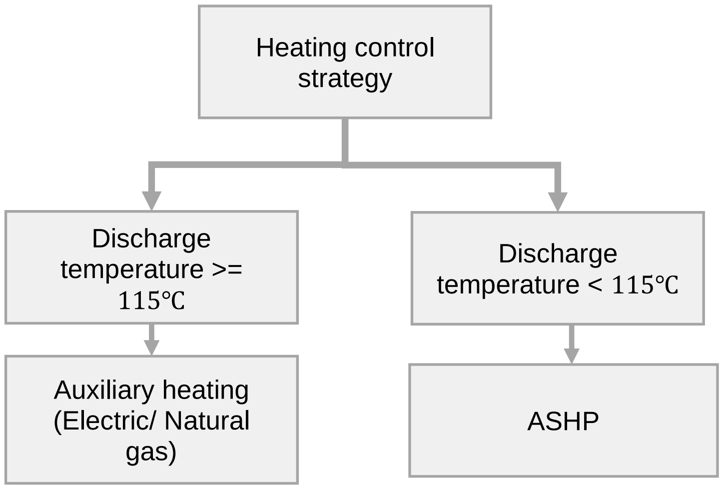

Figure 5: ASHP operation strategy

Provinces like Quebec, Manitoba, and British Columbia harvest their electricity from renewable sources, leading to low GHG emission intensities from the electric grid, which would favor an ASHP retrofit (Asaee et al., 2017).

Table 3: GHG emission comparison

Mode of operation	Annual electricity consumption in MWh	Total natural gas consumption in MWh	GHG emission in tonne	Deviation from natural gas heating
ASHP + electric auxiliary	50.8 24.9-ASHP + 25.9-Electic auxiliary	NA	27.49	+ 38.8%
ASHP + natural gas auxiliary	24.9	30.5	20.8	+ 5.04%
Natural gas	NA	82.6	19.8	NA

The present situation might present an unfavourable case for an ASHP retrofit. However, municipal authorities are working continuously towards adding more renewable energy to the electricity grid, reducing the GHG intensity of the electric grid. For example, if we assume a conservative GHG intensity of the electricity grid as 0.4 kg CO_{2e}/kWh, the emissions from ASHP + natural gas auxiliary for the building under consideration would be 17.28 tonnes of CO_{2e}, which is 13% lower than the natural gas heating system. That is 4.94 kg CO_{2e}/year.m^2 saved using ASHPs. Hence, we can achieve tremendous GHG emission savings using ASHPs.

CONCLUSION

An ASHP is modelled to supply heat to a small office building in Saskatoon, Canada. The operation of ASHP in Saskatoon is challenging because of the harsh cold climate. In a cold environment, ASHP faces the problems of frosting and high discharge temperatures. COP correction factors included in the model account for the frosting and defrosting performance losses. The value of the correction factor depends on the severity of the frosting. The performance and the GHG emission from ASHP operation were investigated in the present study, and the conclusions are as follows:

1. The performance of the ASHP is dependent on ambient temperature and relative humidity. The compression ratio plays a vital role in determining the working envelope and COP of the ASHP
2. Discharge temperature decrease with the decrease in condensation temperature. The operational envelope of an ASHP can be extended to -36^{o}C by operating the ASHP at a condensation temperature of 30^{o}C.
3. The frosting has a significant effect on performance and causes a performance loss of 11% - 20% compared to a no-frost operation
4. The current GHG intensity of the electric grid in Saskatoon does not favour an ASHP retrofit, as retrofit increases the GHG emissions. However, the GHG emission intensity is projected to reduce in the future, selecting ASHP retrofit.

ACKNOWLEDGEMENT

Financial support provided by Research Junction, a collaboration between the City of Saskatoon and the University of Saskatchewan, is gratefully acknowledged. The help provided by Ms. Kathryn Theede, Mr. Chris Richards from the City of Saskatoon, and Dr. Melanie Fauchox (Department of Mechanical Engineering, University of Saskatchewan) is highly appreciated.

Symbols

c: specific heat $\left(\frac{\text{kJ}}{\text{kg.K}}\right)$

Cf: frosting correction factors

COP: coefficient of performance

h: specific enthalpy $\left(\frac{\text{kJ}}{\text{kg}}\right)$

$\dot{\text{m}}$: mass flow rate $\left(\frac{\text{kg}}{\text{s}}\right)$

$\dot{Q}$: heat transfer rate (kW)

T: temperature (K)

Subscripts

a: air

r: refrigerant

comp: compressor

con: condenser

eva: evaporator

exp: expansion valve

in: inlet

o: outlet

REFERENCES

Abergel, T., & Delmastro, *Is cooling the future of heating*? Retrieved July 18, 2022, from https://www.iea.org/commentaries/is-cooling-the-future-of-heating.

Asaee, S. R., Ugursal, V. I., & Beausoleil-Morrison, I. (2017). Techno-economic feasibility evaluation of air to water heat pump retrofit in the Canadian housing stock. *Applied Thermal Engineering*, *vol. 111*, pp. 936–949.

Bertsch, S. S., & Groll, E. A. (2008). Two-stage air-source heat pump for residential heating and cooling applications in northern U.S. climates. *International Journal of Refrigeration*, *vol. 31*, pp. 1282–1292.

Boahen, & Choi. (2019). A Study on the Performance of a Cascade Heat Pump for Generating Hot Water. *Energies*, *vol. 12,* pp. 4313.

Eldeeb, R. (2012) Simulating a heat and moisture transfer panel (HAMP) for maintaining space humidity. M. Sc thesis, University of Saskatchewan, Saskatoon, Canada.

Cabrol, L., & Rowley, P. (2012). Towards low carbon homes - A simulation analysis of building-integrated air-source heat pump systems. *Energy and Buildings*, *vol. 48*, pp. 127–136.

Çengel, Y. a. (2004). Thermodynamics: An Engineering Approach. *McGraw-Hill*.

City of Regina. (2020). *Measuring Energy & Greenhouse Gas*. Retrieved August 18, 2022, from https://www.regina.ca/about-regina/renewable-regina/measuring-energy-greenhouse-gas.

Dong, J., Li, S., Yao, Y., Jiang, Y., Tian, Y., & Tian, H. (2015). Defrosting performances of a multi-split air source heat pump with phase change thermal storage. *International Journal of Refrigeration*, *vol. 55*, pp. 49–59.

Dongellini, M., Piazzi, A., de Biagi, F., & Morini, G. L. The modelling of reverse defrosting cycles of air-to-water heat pumps with TRNSYS; *E3S Web of Conferences, vol.111.*

Ramin, H., Krishnan, E. & Simonson, C.J. (2019). Fixed Bed Regenerators for HVAC Applications, *Symposium on Energy Efficiency in Buildings and Industry, vol. 23,* pp. 1-6.

Hu, B., Yang, D., Cao, F., Xing, Z., & Fei, J. (2015). Hot gas defrosting method for air-source transcritical CO 2 heat pump systems. *Energy and Buildings*, *vol. 86*, pp. 864-872.

Huang, D., Li, Q., & Yuan, X. (2009). Comparison between hot-gas bypass defrosting and reverse-cycle defrosting methods on an air-to-water heat pump. *Applied Energy*, *vol. 86,* pp. 1697–1703.

IEA. (2019). *Heating and Cooling Strategies in the Clean Energy Transition* Retrieved July 18 from https://www.iea.org/reports/heating-and-cooling-strategies-in-the-clean-energy-transition

Jiang, S., Wang, S., Jin, X., & Zhang, T. (2015). A general model for two-stage vapor compression heat pump systems. *International Journal of Refrigeration*, *vol. 51*, pp. 88–102.

Krishnan, E., Ramin, H., & Simonson, C.J. (2019). Performance testing of fixed-bed regenerators for HVAC applications. *Proceedings of the Second Pacific Rim Thermal Engineering Conference*, *Hawai*, USA.

Krishnan, E., Ramin, H., Annadurai, G., Wahab O., A. & Simonson, C.J. (2021). Methodologies for predicting the effectiveness of full-scale fixed-bed regenerators from small-scale test data. *Journal of Thermal Sciences and Engineering Applications*, *vol.12*, p. 051019.

Jiang, S., Wang, S., Jin, X., & Zhang, T. (2015). A general model for two-stage vapor compression heat pump systems. *International Journal of Refrigeration*, *vol. 51*, pp. 88–102.

Li, J., Fan, Y., Zhao, X., Bai, X., Zhou, J., Badiei, A., Myers, S., & Ma, X. (2022). Design and analysis of a novel dual source vapor injection heat pump using exhaust and ambient air. *Energy and Built Environment*, *vol. 3,* pp. 95–104.

Lin, Y., Fan, Y., Yu, M., Jiang, L., & Zhang, X. (2022). Performance investigation on an air source heat pump system with latent heat thermal energy storage. *Energy*, vol. *239*, p. 121898.

Liu, Z., Wang, Y., Xie, Z., Yu, H., & Ma, W. (2017). The related problems and development situation of air source heat pump in the cold and serve cold climate areas. *Procedia Engineering*, *vol. 205*, pp. 368–372.

City of Saskatoon (2019). *Saskatoon's Actions for Climate Change Mitigation.* Retrieved July 18, 2022 from https://www.saskatoon.ca/community-culture-heritage/environment/climate-change

Shao, S., Zhang, H., Fan, X., You, S., Wang, Y., & Wei, S. (2021). Thermodynamic and economic analysis of the air source heat pump system with direct-condensation radiant heating panel. *Energy*, *vol. 225*, p. 120195.

Staffell, I., Brett, D., Brandon, N., & Hawkes, A. (2012). A review of domestic heat pumps. *Energy and Environmental Science*, *vol. 12,* pp. 9291-9306.

Su, W., Li, W., & Zhang, X. (2017). Simulation analysis of a novel no-frost air-source heat pump with integrated liquid desiccant dehumidification and compression-assisted regeneration. *Energy Conversion and Management*, *vol. 148*, pp. 1157–1169.

Sun, S., Guo, H., Lu, D., Bai, Y., & Gong, M. (2021). Performance of a single-stage recuperative high-temperature air source heat pump. *Applied Thermal Engineering*, *vol. 193*, p.116969.

Torcellini, P., Deru, M., Griffith, B., & Benne, K. (2008). DOE Commercial Building Benchmark Models Preprint. *Contract*, *Eia 2005*, http://www.osti.gov/bridge

Yang, L. W., Xu, R. J., Hua, N., Xia, Y., Zhou, W. bin, Yang, T., Belyayev, Y., & Wang, H. S. (2021). Review of the advances in solar-assisted air source heat pumps for the domestic sector. *Energy Conversion and Management*, *vol. 247*, pp. 114710.

Zhao, R., Huang, D., Peng, X., & Qiao, L. (2020). Comprehensive measures to enhance electric heater defrosting (EHD) performance for household frost-free refrigerators. *International Journal of Refrigeration*, *vol. 111*, pp. 1–8.

Zhu, J., Sun, Y., Wang, W., Ge, Y., Li, L., & Liu, J. (2015). A novel Temperature–Humidity–Time defrosting control method based on a frosting map for air-source heat pumps. *International Journal of Refrigeration*, *vol. 54*, pp. 45-54.